Standard-Independent Estimation of Dielectric Permittivity with Microdielectric Fringe-Effect Sensors

ARTICLE *in* ANALYTICAL CHEMISTRY · MARCH 2005

Impact Factor: 5.64 · DOI: 10.1021/ac048723e · Source: PubMed

2 AUTHORS, INCLUDING:

Mikhail Skliar
University of Utah

89 PUBLICATIONS **798** CITATIONS

Anal. Chem. **2005,** *77,* 871−877

Standard-Independent Estimation of Dielectric Permittivity with Microdielectric Fringe-Effect Sensors

Yunn-Hong Choi and Mikhail Skliar*

Department of Chemical Engineering, University of Utah, Salt Lake City, Utah 84112

Microdielectric spectroscopy with planar fringe-effect (FE) interdigital sensors is a useful method for noninvasive characterization of the interfacial properties of the materials. Unfortunately, obtaining an accurate dielectric spectrum is difficult because of the complexity of the probing electrical field created by the FE sensor and the contribution of the sensor substrate and stray elements to the overall measurements. Previously, quantitative microdielectric spectroscopy required the calibration of the FE sensor with standard materials that are known to be dielectrically similar to an unknown sample of interest. This limitation complicates the application of microdielectric spectroscopy, particularly in cases where the monitored sample undergoes a transformation that changes its dielectric permittivity. A standard-independent method for quantitative FE microdielectric measurements is proposed in this paper. The developed method is based on comparison of the theoretically predicted admittance of the FE sensor with the sample of known dielectric properties and the measured sensor admittance. Comparison of the theoretical predictions with the admittance measurements reveals the contribution of the unknown stray elements. The measurements with an unknown sample are then adjusted for the strays. The contribution of the sensor substrate to the sensor measurements is removed using the theoretical model derived from the electroquasistatic approximation of Maxwell equations. The dielectric permittivity of the material being tested is calculated by successively solving the system of complex nonlinear equations for each frequency at which the sensor admittance is measured. The developed method is illustrated by applying it to the dielectric measurements of several dissimilar samples. The results are in excellent agreement with those obtained using the gold standard parallel-plate measurement method over the entire range of frequencies.

Dielectric spectroscopy is an important material characterization method[1] useful in a wide range of applications, including the characterization of polymer relaxation processes,[2−4] phase transition in amorphous, crystalline, and liquid crystalline polymers,[5,6] and chain motion in rodlike polymers.[7] In the traditional approach, the dielectric properties of the material under test (MUT) are obtained by placing a sample between the plates of a parallel-plate (PP) capacitor and measuring the sample's response to the excitation voltage swept over the desired range of frequencies.[8] A more recent alternative to the PP method is to use miniaturized microdielectric fringe-effect (FE) sensors, composed of a set of planar electrodes microfabricated on an insulating substrate, originally proposed by Senturia and Gaverick.[9] With the improvement in microfabrication technology, FE sensors can be manufactured with submicrometer features and integrated into a microdielectrometer chip device, which combines sensing elements with measurement circuitry and data processing. The planar structure and the miniature size of FE sensors make them suitable for noninvasive, interfacial, in situ,[10] and real-time measurements. Spatially resolved and localized measurements are also possible with FE sensors.

Since their introduction, FE sensors have been used in a variety of applications. Examples include the monitoring of moisture and humidity,[11−13] gas,[14,15] chemical,[16] and biological[17,18] sensing, and monitoring of the polymer curing process.[19,20] In these and many

* To whom correspondence should be addressed. E-mail: mikhail.skliar@utah.edu.

(1) Hedvig, P. *Dielectric Spectroscopy of Polymers*; Wiley: New York, 1975.
(2) Adachi, K.; Nishi, I.; Itoh, S.; Kotaka, T. *Macromolecules* **1990**, *23*, 3138−3144.
(3) Boese, D.; Kremer, F. *Macromolecules* **1990**, *23*, 829−835.
(4) Imanishi, Y.; Adachi, K.; Kotaka, T. *J. Chem. Phys.* **1988**, *89*, 7585−7592.
(5) Neagu, R. M.; Neagu, E.; Kyritsis, E.; Pissis, P. *J. Phys. D* **2000**, *33*, 1921−1931.
(6) Wolarz, E.; Kikian, D.; Haase, D.; Bauman, D. *J. Polym. Sci., Part B: Polym. Phys.* **1999**, *37*, 369−377.
(7) McCreight, K. W.; Ge, J. J.; Guo, M.; Mann, I.; Li, F.; Shen, Z.; Jin, S.; Harris, F. W. *J. Polym. Sci., Part B: Polym. Phys.* **1999**, *37*, 1633−1646.
(8) Riande, E.; Saiz, E. *Dipole Moments and Birefringence of Polymers*; Prentice Hall: Upper Saddle River, NJ, 1992.
(9) Senturia, S. D.; Gaverick, S. L. U.S. Patent 4,423,371, 1983.
(10) Senturia, S. D.; Sheppard, N. F.; Lee, H. L.; Day, D. R. *J. Adhes.* **1982**, *15*, 69−90.
(11) Gaverick, S. L.; Senturia, S. D. *IEEE Trans. Electron Devices* **1982**, *29*, 90−94.
(12) Zaretsky, M. C.; Melcher, J. R.; Cooke, C. M. *IEEE Trans. Electron. Insul.* **1989**, *24*, 1167−1175.
(13) Hammann, C.; Kampfrath, G.; Mueller, M. *Sens. Actuators, B* **1991**, *1*, 142−147.
(14) Kolesar, E. S.; Wiseman, J. M. *Anal. Chem.* **1989**, *61*, 2355−2361.
(15) Endres, H. E.; Drost, S. *Sens. Actuators, B* **1994**, *22*, 7−11.
(16) Zhou, R.; Hiermann, A.; Schierbaum, K. D.; Geckeler, K. E.; Göpel, W. *Sens. Actuators, B* **1995**, *24−25*, 443−447.
(17) Sangodkar, H.; Sukeerthi, S.; Srinivasa, R. S.; Lai, R.; Contractor, A. Q. *Anal. Chem.* **1996**, *68*, 779−783.
(18) Sergeyeva, T. A.; Lavrix, N. V.; Rachkov, A. E.; Kazantseva, Z. I.; Piletsky, S. A.; Elskaya, A. V. *Anal. Chim. Acta* **1999**, *391*, 289−297.

10.1021/ac048723e CCC: $30.25
Published on Web 12/31/2004

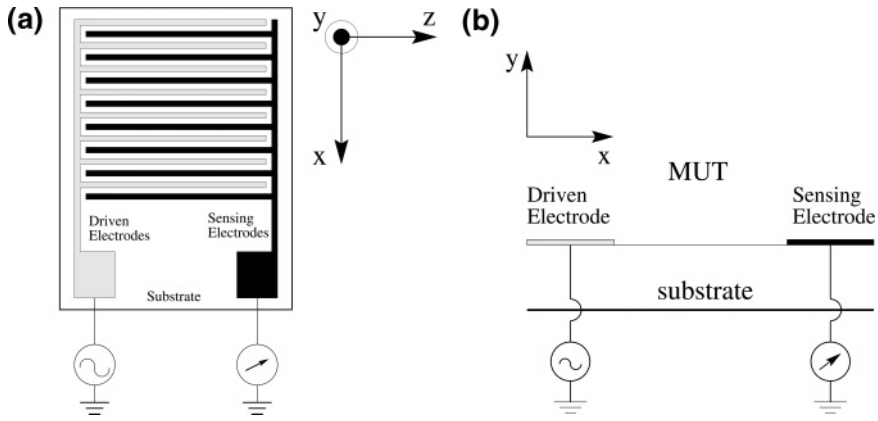

Figure 1. Top (a) and cross-sectional (b) views of the FE sensor. For clarity, the total number of electrode pairs is reduced. The MUT sample is placed on top of the electrodes. The excitation potential is applied to the driven electrodes while the resulting current is measured at the sensing electrodes.

other applications, FE measurements are used to monitor a change in the dielectric properties of the MUT. At the same time, only a few dielectric spectroscopy studies have been performed[21,22] because of the difficulty in obtaining quantitative dielectric measurements with FE sensors. A summary of the factors that complicate the quantitative estimation of the dielectric properties based on FE measurements is given in a recent study,[23] which also reviewed the available calibration method for quantitative FE measurements. A novel method for quantitative dielectroscopic measurements over a broad range of frequency, proposed in ref 23, requires the calibration of a FE sensor using two samples with known dielectric spectra. It was shown to be superior to the alternatives, but as it was pointed out, the accuracy of the dielectric measurements depends on the selected calibration standards. Specifically, to guarantee highly accurate dielectric measurements, the calibration must be performed with the standard materials dielectrically similar to an unknown sample.

The method proposed in the current paper removes the dependence of the estimated dielectric permittivities, obtained based on the admittance measurements of the FE sensor, on the standards-dependent calibration. The developed standard-free calibration method is based on the comparison of the theoretically predicted admittance of the FE sensor with a sample of known dielectric properties to the measured sensor admittance. The inverse problem of estimating dielectric permittivities of unknown samples from the admittance measurements of the FE sensor is formulated as an eigenvalue problem, as suggested in ref 24. Application of the developed method is illustrated by applying it to the dielectric measurements of several dissimilar samples. The results are in excellent agreement with those obtained using the gold standard PP measurement method over the entire range of frequencies.

THEORY

Figure 1 schematically depicts a typical FE sensor. For sufficiently low frequency of the excitation voltage, the electroquasistatic electric field, **E**, of a FE sensor can be described by the following equation:

$$\nabla\cdot(\epsilon^*\mathbf{E}) = 0 \tag{1}$$

where $\epsilon^* = \epsilon' - j\epsilon''$ is the dielectric permittivity and ϵ' and ϵ'' are the dielectric storage and loss components, respectively. Equation 1 is derived from Maxwell's equations as shown in section A of the Supporting Information. Since the electric field can be expressed as $\mathbf{E} = -\nabla\varphi$, where φ is the potential, we conclude that, for a homogeneous MUT and sensor substrate, the potential distribution is described by the Laplace equation, $\nabla^2\varphi = 0$, which we wish to solve with following boundary conditions:

1. The potential of the driven electrodes is $\varphi_d = |\varphi_d| \exp(j\omega t)$. The sensing electrodes are maintained at zero potential.

2. The bottom of the sensor substrate is grounded: $\varphi(x, -T_{sub}, z) = 0$, where T_{sub} is the thickness of the sensor substrate.

3. Symmetry boundary conditions $\partial\varphi/\partial x = 0$ are imposed at the centerlines of the driven and sensing electrodes.

4. A semi-infinitely thick MUT layer is placed on the top of the FE sensor.

The last boundary condition is a good approximation when the thickness of the MUT sample is finite but large compared to the spacing between the planar electrodes of the sensor. If we assume a two-dimensional potential distribution, which is a reasonable assumption for FE sensors with a high ratio of electrode length to width, the analytical solution of the Laplace equation can be obtained:

$$\varphi(x, y) = \begin{cases} \varphi^{mut} = \varphi(x, y \geq 0) = \sum_{n=0}^{\infty} f_n \exp(-k_n y) \cos(k_n x) \\ \varphi^{sub} = \varphi(x, y \leq 0) = \sum_{n=0}^{\infty} f_n \dfrac{\sinh[k_n(y + T_{sub})]}{\sinh(k_n T_{sub})} \cos(k_n x) \end{cases} \tag{2}$$

where the superscripts mut and sub are used to denote the

(19) Senturia, S. D.; Sheppard, N. F.; Poh, S. Y.; Appelman, H. R. *Polym. Eng. Sci.* **1981**, *21*, 113−118.
(20) Sheppard, N. F.; Day, D. R.; Lee, H. L.; Senturia, S. D. *Sens. Actuators* **1982**, *2*, 263−274.
(21) Senturia, S. D.; Sheppard, N. F. *Adv. Polym. Sci.* **1986**, *80*, 1−47.
(22) Hill, D. A.; Fodor, J. S. *Polym. News* **1996**, *21*, 189−196.
(23) Choi, Y.; Skliar, M. *Anal. Chem.* **2004**, *76*, 4143−4149.
(24) Lesieutre, B. C.; Mamishev, A. V.; Du, Y.; Keskiner, E.; Zahn, M. *IEEE Trans. Dielectr. Electron. Insul.* **2001**, *8*, 577−588.

solution in MUT and sensor substrate regions with the interface at $y = 0$, f_n are the Fourier coefficients, $k_n = n\pi/L$, and L is the distance between the centerlines of driven and sensing electrodes. Note that (2) is derived by ignoring the height of the electrodes in the y direction, which for practical devices is very small relative to other sensor dimensions and has a negligible effect on the solution.

The x and y components of the electric field in the MUT and the substrate are now obtained by taking the negative gradient of φ:

$$E_x(x, y) = \begin{cases} E_x^{\text{mut}}(x, y \geq 0) = \sum_{n=0}^{\infty} k_n f_n \exp(-k_n y) \sin(k_n x) \\ E_x^{\text{sub}}(x, y \leq 0) = \sum_{n=0}^{\infty} k_n f_n \dfrac{\sinh[k_n(y + T_{sub})]}{\sinh(k_n T_{\text{sub}})} \sin(k_n x) \end{cases} \quad (3)$$

$$E_y(x, y) = \begin{cases} E_y^{\text{mut}}(x, y \geq 0) = \sum_{n=0}^{\infty} k_n f_n \exp(-k_n y) \cos(k_n x) \\ E_y^{\text{sub}}(x, y \leq 0) = \sum_{n=0}^{\infty} -k_n f_n \dfrac{\cosh[k_n(y + T_{\text{sub}})]}{\sinh(k_n T_{\text{sub}})} \cos(k_n x) \end{cases} \quad (4)$$

where the complex coefficients f_n are yet to be determined. Equations 2−4 indicate that both the potential and the electric field decay exponentially in the positive and negative directions normal to the interface of the sensor's substrate and MUT. This last observation justifies the use MUT samples with finite thickness in practical application of the method.

Potential Profile On the Interface. The Fourier coefficients, f_n, in solutions 2−4 satisfy the following integral equations[25]:

$$f_0 = \frac{1}{L}\int_0^L \varphi(x, y = 0)\, dx = \frac{|\varphi_d|}{L}\int_0^L \varphi_0(x)\, dx$$

$$f_n = \frac{2}{L}\int_0^L \varphi(x, y = 0) \cos(k_n x)\, dx = \frac{2|\varphi_d|}{L}\int_0^L \varphi_0(x) \cos(k_n x)\, dx \quad (5)$$

where φ_0 is the complex normalized potential:

$$\varphi_0(x) = \varphi(x, y = 0)/|\varphi_d|$$

At $y = 0$, the profile of φ should be such that the potentials of the driven and sensing electrodes are, correspondingly, $|\varphi_d|$ and 0. As suggested in ref 26, we can satisfy this requirement by assuming the following piecewise linear interfacial potential:

$$\varphi_0(x) = \begin{cases} 1 & 0 \leq x \leq x_0 \\ \varphi_0(x_i)\dfrac{(x - x_{i-1})}{x_i - x_{i-1}} - \varphi_0(x_{i-1})\dfrac{(x - x_i)}{x_i - x_{i-1}} & x_{i-1} < x < x_i \\ 0 & x_{k+1} \leq x \leq L \end{cases} \quad (6)$$

where $\varphi_0(x_i)$ is an unknown normalized potential in the following k collocation points uniformly distributed at the interface:

$$x_i = \frac{L}{2(k + 1)} i + \frac{L}{4},\ i = 1, ..., k$$

With the assumed parametrization of the interfacial potential, for the first $m + 1$ Fourier coefficients, the system of eqs 5 can be written in the vector form as

$$\mathbf{F} = |\varphi_d|[\mathbf{M}\Phi] \quad (7)$$

where the complex vectors $\mathbf{F}$ and Φ are defined as

$$\mathbf{F} = [f_0, f_1, f_2, ..., f_{m-1}, f_m]^T \quad (8)$$

$$\Phi = [1, \varphi_0(x_1), \varphi_0(x_2), ..., \varphi_0(x_{k-1}), \varphi_0(x_k)]^T \quad (9)$$

and the elements of the real matrix $\mathbf{M} \in \mathscr{P}^{(m+1)(k+1)}$ are equal to

$$M_{1,1} = (1/2L)(x_0 + x_1)$$

$$M_{1,i+1} = (1/2L)(x_{i+1} - x_{i-1})$$

$$M_{n+1,1} = \frac{2}{L}\left[\frac{\cos(k_n x_0) - \cos(k_n x_1)}{k_n^2 (x_1 - x_0)}\right]$$

$$M_{n+1,i+1} = \frac{2}{Lk_n^2}\left[\frac{\cos(k_n x_i) - \cos(k_n x_{i-1})}{x_i - x_{i-1}} - \frac{\cos(k_n x_{i+1}) - \cos(k_n x_i)}{x_{i+1} - x_i}\right] \quad (10)$$

where $n = 1, ..., m$. To calculate the potential values at the interface, Φ, we first note that eq 1 implies that at the interface

$$\epsilon_{\text{mut}}^* E_y^a - \epsilon_{\text{sub}}^* E_y^b = 0 \quad (11)$$

where $E_y^a(x) = E_y(x, 0^+) = E_y^{\text{mut}}(x, y = 0)$, and $E_y^b(x) = E_y(x, 0^-) = E_y^{\text{sub}}(x, y = 0)$. The piecewise linear parametrization of the interfacial potential implies a piecewise constant profile of the electric field with discontinuities in the collocation points. To avoid the ambiguity of the solution in the points of discontinuity, following,[26] eq 11 is rewritten in the integral form

$$\int_{x_i + x_{i-1}/2}^{x_{i+1} + x_i/2} [\epsilon_{\text{mut}}^* E_y^a(x) - \epsilon_{\text{sub}}^* E_y^b(x)]\, dx = 0 \quad (12)$$

for each $i = 1, ..., k$. After calculating the electric field corresponding to the parametrization (6) and integration, eq 12 can be written in the following vector form:

(25) Kreyszig, E. *Advanced Engineering Mathematics*; Wiley: New York, 1988; pp 593−594.
(26) Zaretsky, M. C.; Mouayad, L.; Melcher, J. R. *IEEE Trans. Electron. Insul.* **1988**, *23*, 897−917.

$$[\epsilon^*_{\text{sub}}\mathbf{B} + \epsilon^*_{\text{mut}}\mathbf{A}]\mathbf{F} = |\varphi_{\text{d}}|[\epsilon^*_{\text{sub}}\mathbf{BM} + \epsilon^*_{\text{mut}}\mathbf{AM}]\Phi = 0_1 \quad (13)$$

where 0_1 is the $k \times 1$ zero vector, and the elements of the real matrices $\mathbf{A} \in \mathcal{R}^{k\times(m+1)}$ and $\mathbf{B} \in \mathcal{R}^{k\times(m+1)}$ are equal to

$$A_{i,n+1} = \sin\left(k_n \frac{x_{i+1} + x_i}{2}\right) - \sin\left(k_n \frac{x_i + x_{i-1}}{2}\right) \quad (14)$$

$$B_{i,n+1} = \coth(k_n T_{\text{sub}})\left[\sin\left(k_n \frac{x_{i+1} + x_i}{2}\right) - \sin\left(k_n \frac{x_i + x_{i-1}}{2}\right)\right] \quad (15)$$

for each $n = 0, ..., m$. With known dielectric properties of ϵ^*_{mut} and ϵ^*_{sub}, the k complex equations of system 13 can be used to solve for k unknown components of the complex vector Φ. The unknown Fourier coefficients are then calculated according to eq 7.

Predicting Sensor Admittance. The electrical equivalent circuit of the FE sensor is shown in Figure 2. $\mathbf{Y}_{\text{sam}}$ and $\mathbf{Y}_{\text{sub}}$ are the components of the sensor admittance corresponding to the contribution of the MUT and the sensor substrate, respectively. The overall admittance of the sensor, $\mathbf{Y}_{\text{sen}} = \mathbf{Y}_{\text{sam}} + \mathbf{Y}_{\text{sub}}$, can be obtained as follows (cf. eq 4 of ref 23):

$$\mathbf{Y}_{\text{sen}} = \frac{I}{\varphi_{\text{d}}} = \frac{I_{\text{sam}}}{\varphi_{\text{d}}} + \frac{I_{\text{sub}}}{\varphi_{\text{d}}} = \frac{j\omega\epsilon_0 N_{\text{e}} L_{\text{sen}}}{|\varphi_{\text{d}}|}\int_{3L/4}^{L}[\epsilon^*_{\text{sub}} E^b_y - \epsilon^*_{\text{mut}} E^a_y]\, \text{d}x \quad (16)$$

where N_e is the total number of all sensing and driven electrodes, L_{sen} is the length of the electrode in the z direction, and ϵ_0 is the dielectric constant of free space. Using the obtained solution for the electric field and potential distribution, after integration, the last equation can be written in the following form:

$$\mathbf{Y}_{\text{sen}} = \frac{j\omega\epsilon_0 N_{\text{e}} L_{\text{sen}}}{|\varphi_{\text{d}}|}[\epsilon^*_{\text{sub}}\mathbf{D} + \epsilon^*_{\text{mut}}\mathbf{C}]\mathbf{F} = j\omega\epsilon_0 N_{\text{e}} L_{\text{sen}}[\epsilon^*_{\text{sub}}\mathbf{DM} + \epsilon^*_{\text{mut}}\mathbf{CM}]\Phi \quad (17)$$

where the elements of vectors $\mathbf{C} \in \mathcal{R}^{1\times(m+1)}$ and $\mathbf{D} \in \mathcal{R}^{1\times(m+1)}$ are equal to

$$C_{1,n+1} = \sin(k_n(3L/4)) \quad (18)$$

$$D_{1,n+1} = \coth(k_n T_{\text{sub}})\, \sin(k_n(3L/4)) \quad (19)$$

Equation 17 gives the theoretical prediction of the admittance of the FE sensor of a given geometrical design and known dielectric permittivities of the substrate and the semi-infinite MUT sample.

Stray Impedance. The equivalent circuit of Figure 2 includes the contribution of the stray impedance $\mathbf{Z}_{\text{stray}}$, usually introduced by the interconnecting leads, connection fixture, contact impedance, the FE sensor itself, and other unknown factors. Given the measurements of the FE sensor admittance, $\mathbf{Y}_m$, and using the theoretical prediction of $\mathbf{Y}_{\text{sen}}$, the stray impedance can be estimated as

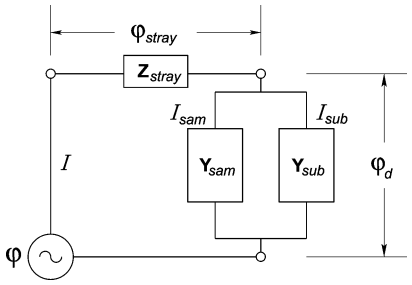

Figure 2. Equivalent circuit of the FE sensor.

$$\mathbf{Z}_{\text{stray}} = R_{\text{stray}} + jX_{\text{stray}} = \left[\frac{1}{\mathbf{Y}_m} - \frac{1}{\mathbf{Y}_{\text{sen}}}\right] \quad (20)$$

where $\mathbf{Y}_m = 1/R_m + j\omega C_m$ and $C_m(\omega)$ and $R_m(\omega)$ are the corresponding capacitance and resistance of the FE sensor in the parallel equivalent circuit.

Even for the FE sensors of identical design, the microfabrication process and the electrical connections may introduce an unknown and different variability of the sensor characteristics. Therefore, it is advisable to calculate the series stray impedance once for every new FE sensor put in service. With known dielectric permittivity of the sensor substrate, the estimation of $\mathbf{Z}_{\text{stray}}$ requires a single measurement of $\mathbf{Y}_m$ with a "thick" (relative to electrode spacing L) MUT sample of known permittivity so that $\mathbf{Y}_{\text{sen}}$ can be calculated. The measurements with the vacuum sample ($\epsilon^*_{\text{mut}} = 1$), closely approximated by dry air, are most convenient in estimating stray contributions. However, since $\mathbf{Z}_{\text{stray}}$ is MUT independent, any sample with known ϵ^*_{mut} can be used in stray estimation.

Dielectric Permittivity of MUT. Our main interest is the estimation of the dielectric permittivity of an unknown sample based on FE admittance measurements. The combination of eqs 13 and 17 yields the following system of $k + 1$ complex equations nonlinear in $k + 1$ complex unknowns:

$$\begin{bmatrix}\epsilon^*_{\text{sub}}\mathbf{BM} + \epsilon^*_{\text{mut}}\mathbf{AM} \\ \epsilon^*_{\text{sub}}\mathbf{DM} + \epsilon^*_{\text{mut}}\mathbf{CM}\end{bmatrix}\Phi = \begin{bmatrix}0_1 \\ \mathbf{Y}'_m\end{bmatrix} \quad (21)$$

where the complex scalar $\mathbf{Y}'_m$ is the stray-adjusted admittance at a given frequency equal to

$$\mathbf{Y}'_m = \frac{[1/\mathbf{Y}_m - \mathbf{Z}_{\text{stray}}]^{-1}}{j\omega\epsilon_0 N_{\text{e}} L_{\text{sen}}} = \frac{\mathbf{Y}_{\text{sen}}}{j\omega\epsilon_0 N_{\text{e}} L_{\text{sen}}} \quad (22)$$

The unknown complex ϵ^*_{mut} and k unknown complex components of Φ can now be found from eq 21 using iterative root-finding methods. Alternatively, in the generalized eigenvalue formulation,[24] preferable from the numerical standpoint, eq 21 is rewritten as

$$\left(\mathbf{P} - \epsilon^*_{\text{mut}}\begin{bmatrix}-\mathbf{AM} \\ -\mathbf{CM}\end{bmatrix}\right)\Phi = 0_2 \quad (23)$$

where 0_2 is the $(k + 1)$ zero vector, and

$$\mathbf{P} = \epsilon^*_{\text{sub}} \begin{bmatrix} \mathbf{BM} \\ \mathbf{DM} \end{bmatrix} - \begin{bmatrix} 0 & \cdots & 0 \\ \cdot & \cdots & \cdot \\ 0 & \cdots & \cdot \\ \mathbf{Y}'_m & \cdots & 0 \end{bmatrix} \tag{24}$$

Equation 23 has $k + 1$ solutions of which only one gives a physically meaningful value of ϵ^*_{mut}. The components of the generalized eigenvector Φ, corresponding to the physical solution ϵ^*_{mut}, after scaling that makes Φ's first entry equal to $|\varphi_d|$, give the potential profile at the interface $y = 0$ in all collocation points. The scaling is necessary since eigenvectors are unique only to a scalar multiplier.

PROPOSED METHOD

The following steps summarize the proposed method for quantitative FE measurements of the dielectric permittivity of a MUT. Assuming that the permittivity of the sensor substrate is known, perform the steps below.

1. For each new FE sensor put into service, estimate the contribution of stray components, $\mathbf{Z}_{\text{stray}}$: (a) Use the FE sensor to measure the frequency-dependent admittance $\mathbf{Y}_m = \mathbf{Y}_m(\omega)$ with a sample of known permittivity. Measurements with dry air, for which ϵ^*_{mut} is equal to ~1, are usually convenient. However, any sample with known permittivity (e.g., measured using gold standard PP method) can be used as long as the thickness of the sample is ~$2L$ or larger. (b) Given the sensor geometry, and the dielectric properties, ϵ^*_{mut} and ϵ^*_{sub}, use eq 17 to calculate the theoretical value of the sensor admittance, $\mathbf{Y}_{\text{sen}}$, where Φ is found from eq 13. (c) Use eq 20 to calculate $\mathbf{Z}_{\text{stray}}$. Save the estimated value of stray contributions for future use with unknown samples.

2. Use the FE sensor to measure the admittance $\mathbf{Y}_m(\omega)$ with an unknown MUT sample over the frequencies of interest, ω_i, $i = 1, 2, \ldots$.

3. Use eq 22 to compensate the measurements for the stray contributions.

4. For $\mathbf{Y}'_m(\omega_1)$, solve the system of complex eqs 21, nonlinear in unknown Φ and ϵ^*_{mut}. The solution can be found as a solution of the generalized eigenproblem 23 (a numerically preferred approach for which reliable software is available) or by direct iterative root finding. In either case, a single physical result must be selected out of the possible multiple solutions.

5. Repeat the above step for all remaining measurements $\mathbf{Y}'_m(\omega_i)$.

The described procedure results in the desired estimation of the permittivity spectra $\epsilon^*_{\text{mut}}(\omega)$ of an unknown sample, and the potential profile $\Phi(\omega)$ at the sensor−MUT interface, which may be of separate interest. An important improvement over the methods discussed in ref 23 is that the calibration of the FE sensor with the known sample, dielectrically similar to an unknown MUT is no longer required. The pseudocode of the algorithm implementing the proposed method is given in the Supporting Information, section B.

EXPERIMENTS

Materials. Two commercially available (Sigma-Aldrich) liquid *cis*-polyisoprene (*cis*-PI) samples used in the present study are the same as those utilized in ref 23. The first *cis*-PI sample, PI-38, obtained by depolymerization of natural rubber, is a brown viscous liquid at room temperature with the average molecular weight of ~38 000. The second *cis*-PI sample, PI-40, has an average molecular weight of 40 000, appears as a viscous yellow liquid at room temperature, and is obtained by depolymerization of synthetic *cis*-1,4-polyisoprene rubber. The third dielectrically dissimilar sample used in this study is the commercially available vegetable cooking oil (canola oil)—a chemically complex and poorly characterized material. This third sample is included to demonstrate that the proposed standard-independent procedure produces accurate results for dissimilar materials.

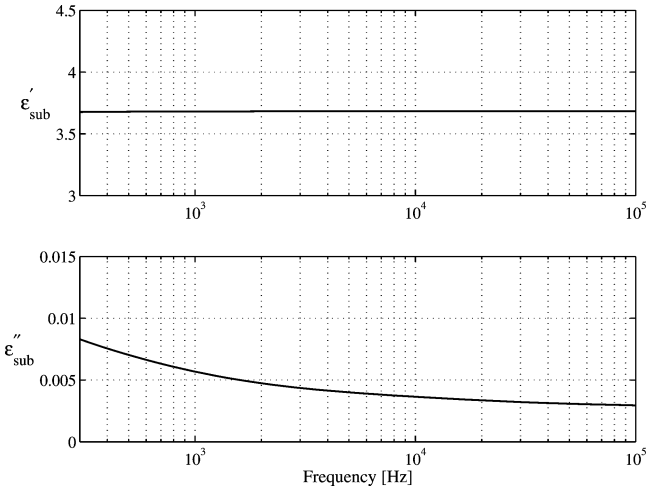

Figure 3. Dielectric properties of the sensor substrate obtained using the PP method.

Dielectric Measurements. The FE measurements were accomplished with the commercially available FE sensor (MS-05, Micromet Instruments), which has a 5-μm spacing between the electrodes. The sensor consists of a periodic pattern of interdigitated chromium electrodes of equal width and spacing, microfabricated on an insulating quartz substrate. The sensor has approximately 340 electrodes, each 5 μm wide and 7.6 mm long. The MUT sample was placed on the top of the FE sensor, which was connected to HP4284A precision LCR meter using a custom-made connection fixture. The measurements were then made at room temperature with the frequency sweep from 300 to 10^5 Hz.

The dielectric permittivity, $\epsilon^*_{\text{sub}}(\omega)$, of the MS-05 sensor substrate was estimated experimentally. One MS-05 sensor was sacrificed by vacuum sputtering chromium onto both sides of the substrate to form a PP capacitor. The admittance of the resulting capacitor was then measured, and the corresponding dielectric storage and loss spectra of the substrate were estimated using the standard equations for the PP method. The obtained dielectric storage and loss spectra of the sensor substrate, subsequently used in estimating $\epsilon^*_{\text{mut}}(\omega)$ of the three considered MUT samples, are shown in Figure 3.

To assess the accuracy of the estimated dielectric permittivity of the MUT based on microdielectric measurements, the FE results were compared with those obtained using the gold standard PP measurement method. The PP measurements were carried out using HP16452A liquid test fixture. The frequency-dependent admittance measurements, expressed in terms of C_m and R_m components of a parallel equivalent circuit, were obtained

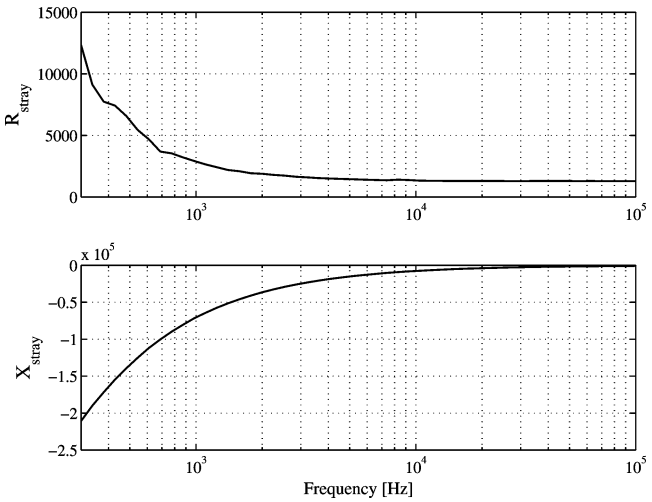

Figure 4. Estimated series stray impedance of the FE sensor obtained by comparing the theoretical predictions to the measurements of the sensor admittance with air as a standard material.

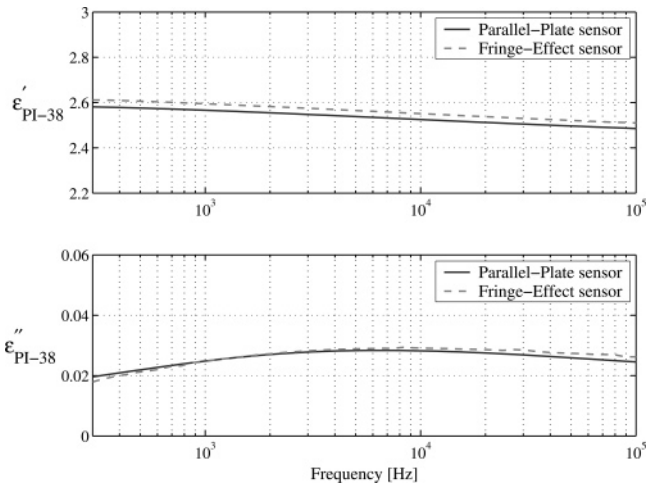

Figure 5. Dielectric storage and loss of the PI-38 sample estimated using FE and PP measurements.

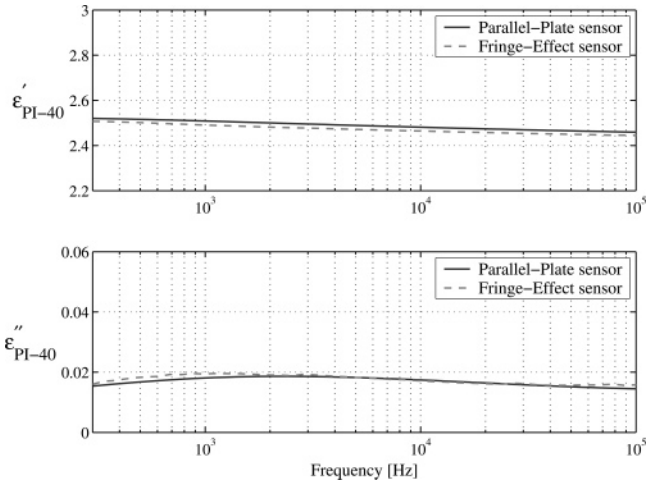

Figure 6. Dielectric storage and loss of the PI-40 sample estimated using FE and PP measurements.

by applying a sweep frequency to the PP sensor and recording the response with HP4284A meter. The PP measurements were compensated for unknown disturbances (strays) using the standard short and open compensation methods following the manufacturer's recommendations. The effect of the fringing electric field on the edges of the PP sensor plates was compensated according to the procedure, suggested by the manufacturer. The PP measurements were then used to calculate the complex dielectric spectra of the sample.

The PP and FE measurements were made under the same environmental conditions. The data acquisition was automated using Agilent's VEE graphical programming software.

RESULTS

Using air as a standard material ($\epsilon^*_{mut}(\omega) = 1$ assumed), the stray impedance $\mathbf{Z}_{stray}$ was estimated as described in step 1 of the proposed method. The results, shown in Figure 4 as the real and the imaginary parts of the stray impedance, were saved and later used in subsequent experiments to obtain the adjusted admittance, $\mathbf{Y}'_m$, according to eq 22. It is advisable to perform the stray compensation procedure once for each FE sensor put into service, even when replacing a sensor of identical design and specifications.

The adjusted admittance measurements with each unknown sample were used to estimate the dielectric permittivities of the MUT following steps 4 and 5 of the proposed procedure. Figures 5−7 show the results for PI-38, PI-40, and the oil samples based on FE measurements in the form of the estimated dielectric storage and loss spectra. For comparison, these figures also depict the results obtained using the gold standard PP method. For all samples, $\mathbf{Z}_{stray}$ depicted in Figure 4 was used in calculation of the dielectric loss and storage spectra.

DISCUSSION AND CONCLUSION

The recently proposed method[23] for the quantitative microdielectric measurements with the FE sensors allows for the separation of the contribution of the sensor substrate and stray components from the contribution of interest made by the MUT sample. However, to achieve highly accurate measurements of the dielectric spectra, it was noted that the FE sensor must be calibrated with two samples of known dielectric permittivity. Furthermore, it was pointed out that the calibration samples must be dielectrically similar to an unknown sample to guarantee highly accurate results. The requirement of the calibration with samples dielectrically similar to the unknown MUT is a limitation. It complicates or even rules out the microdielectric characterization of the materials undergoing dynamic transformations that affect their dielectric properties. FE measurements of the dielectric properties during the polymerization reaction is one example for which it may be difficult to obtain quantitative measurements following previously developed methods.

In the present paper, we develop and test the standard-independent method for quantitative microdielectric measurements. A single and arbitrarily selected sample with known dielectric loss and storage spectra is needed to estimate the contribution of unknown strays to the FE measurements. Specifically, given the FE sensor geometry and the dielectric properties of a standard sample and the sensor substrate, the theoretical prediction of the sensor admittance can be made. The comparison with the admittance measurements then reveals the contribution of the unknown stray elements. The measurements with an unknown sample are then adjusted for the stray contributions.

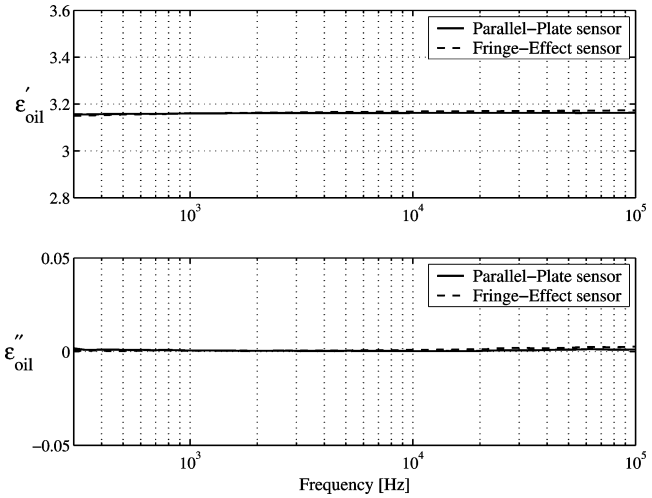

Figure 7. Dielectric storage and loss of the vegetable oil sample estimated using FE and PP measurements.

The contribution of the sensor substrate to the sensor admittance is removed using the theoretical model derived from the electroquasistatic approximation of Maxwell equations, and the dielectric permittivity of the MUT is calculated by successively solving the system of complex nonlinear equations for each frequency at which the sensor admittance is measured.

The numerical complexity is the disadvantage of the developed method compared to the alternative.[23] The numerical issues can be mitigated by reformulating the root finding problem as the generalized eigenvalue problem,[24] for which reliable numerical solvers are readily available. Unfortunately, when the microdielectric measurements are made with an FE sensor other than the regular interdigital type (such as sensors that create essentially three-dimensional potential and field distributions), the numerical complexity of the proposed method will be further complicated. The main advantage of the developed method is in its independence on the dielectric properties of the calibration standards, which allows for its utilization in the applications where the dielectric properties of an unknown sample are either entirely unknown or changing with time. Higher frequency measurements of the dielectric properties can be performed essentially in real time. The rate of low-frequency measurements is fundamentally constrained by the period of the excitation signal equal $2\pi/\omega$.

The developed method requires that the dielectric properties of the FE sensor substrate are known. Such an assumption may not be adequate in some applications. For example, the FE sensor may be a part of a more complex microelectronic device, produced in a multistep microfabrication process, which may introduce a variability of the substrate onto which the FE electrodes are incorporated using chemical or physical deposition methods, followed by patterning and etching. If the properties of the substrate are unknown, the proposed method can be modified to first estimate $\epsilon^*_{sub}(\omega)$ by solving eq 21 with unadjusted measurements $\mathbf{Y}_m(\omega_i)$, where $\mathbf{Y}_m$ is obtained with the MUT sample of known permittivity. Once ϵ^*_{sub} is calculated, the permittivity of unknown samples can be estimated following steps 2−5 of the proposed method. Note, however, that the described modification of the proposed approach uses a single element $\mathbf{Y}_{sub}$ (Figure 2) to capture the combined effect of the stray elements $\mathbf{Z}_{stray}$ and the sensor substrate. Consequently, the estimated $\epsilon^*_{sub}(\omega)$ may not be physically meaningful (i.e., it may indicate negative loss, storage, or both). Despite potential problems in arriving at an accurate value of the unknown ϵ^*_{sub}, the experimental evidence (not included in this paper) indicates that the modified approach usually leads to an accurate estimation of the true permittivity of the MUT sample of interest when compared to the PP results.

The application of the proposed method of the quantitative microdielectric measurements is demonstrated by estimating the permittivity spectra of dielectrically dissimilar samples. The comparison with the results obtained using the gold standard PP method shows an excellent agreement and the independence FE microdielectric measurements on the dielectric properties of the calibration standard.

ACKNOWLEDGMENT

This research was supported by the National Science Foundation (CAREER Grant CTS-9875462) and the Center for Biopolymers at Interfaces at the University of Utah.

Received for review August 26, 2004. Accepted November 8, 2004.

AC048723E